

Adversarial Sparsity Attacks on Deep Neural Networks

Sarada Krithivasan, Sanchari Sen and Anand Raghunathan
 School of Electrical and Computer Engineering, Purdue University
 {skrithiv, sen9, raghunathan}@purdue.edu

Abstract—Adversarial attacks have exposed serious vulnerabilities in Deep Neural Networks (DNNs) through their ability to force misclassifications through human-imperceptible perturbations to DNN inputs. We explore a new direction in the field of adversarial attacks by suggesting attacks that aim to degrade the computational efficiency of DNNs rather than their classification accuracy. Specifically, we propose and demonstrate sparsity attacks, which adversarially modify a DNN’s inputs so as to reduce sparsity (or the presence of zero values) in its internal activation values. Exploiting sparsity in hardware and software has emerged as a popular approach to improve DNN efficiency in resource-constrained systems. The proposed attack increases the execution time and energy consumption of sparsity-optimized DNN implementations, raising concern over their deployment in latency and energy-critical applications.

We propose a systematic methodology to generate adversarial inputs for sparsity attacks by formulating an objective function that quantifies the network’s activation sparsity, and minimizing this function using iterative gradient-descent techniques. To prevent easy detection of the attack, we further ensure that the perturbation magnitude is within a specified constraint and that the perturbation does not affect classification accuracy. We launch both white-box and black-box versions of adversarial sparsity attacks on image recognition DNNs and demonstrate that they decrease activation sparsity by 1.16x-1.82x. On a sparsity-optimized DNN accelerator, the attack results in degradations of 1.12x-1.59x in latency and 1.18x-1.71x in energy-delay product (EDP). Additionally, we analyze the impact of various hyper-parameters and constraints on the attack’s efficacy. Finally, we evaluate defense techniques such as activation thresholding and input quantization and demonstrate that the proposed attack is able to withstand them, highlighting the need for further efforts in this new direction within the field of adversarial machine learning.

I. INTRODUCTION

The widespread success of Deep Neural Networks (DNNs) in various machine learning applications, including image recognition, speech recognition, and natural language processing, has led to their deployment in several real-world products and services [1]–[3]. State-of-the-art DNNs place immense computational and memory demands on the underlying computing platforms on which they execute. Consequently, a wide range of algorithmic, software and hardware techniques have been proposed to improve the execution efficiency of DNNs.

Several recent efforts optimize DNN implementations by exploiting *sparsity*, or the prevalence of zero values in DNN

weights and activations, to optimize storage and computation. For example, sparsity-optimized DNN implementations may store the sparse data-structures in a compact format to reduce the memory requirements [4] and/or skip redundant multiply-accumulate operations caused by zero-valued operands to reduce their computational requirements [5]–[11]. We observe that, in sparsity-optimized platforms, the execution time and energy consumption of DNNs are strongly dependent on the amount of sparsity present in the networks. Figure 1 depicts the variation in latency of a sparsity-aware hardware accelerator [6] when evaluated on the ImageNet dataset for the VGG16 [12] network. As can be seen, increasing (decreasing) the activation sparsity leads to proportional decreases (increases) in latency.

We leverage the aforementioned property to expose a vulnerability of sparsity-optimized DNN implementations. Specifically, we present an attack that adversarially perturbs the input so as to significantly reduce sparsity in the internal activations of the network. This greatly diminishes or eliminates the benefits of sparsity optimizations, and leads to *unanticipated increases in inference latency and energy consumption*.

For example, an autonomous self-driving car is expected to detect obstacles or unforeseen changes in the environment within around 600 milliseconds [13]. In that time, the Cnvlutin accelerator can

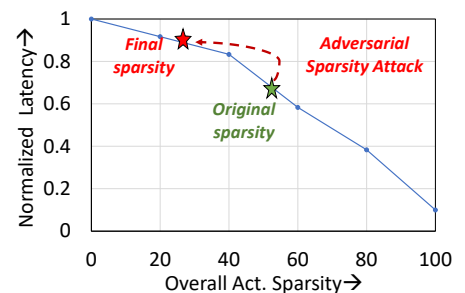


Fig. 1: Impact of activation sparsity on latency

process nearly 30 frames using the VGG16 DNN, assuming an average activation sparsity of 45-50%. However, under the influence of the attack (detailed results are presented in Section VI), the average activation sparsity decreases by 1.79 \times and the latency of the accelerator is increased by nearly 1.4 \times , causing it to process only 21 frames in the available time. The DNN could thus miss potentially critical data present in the remaining frames. For ensuring correct real-time operation, such an attack would require designers to over-design systems, essentially losing the benefits from sparsity optimization. The increased energy consumption resulting from sparsity attacks could also potentially lead to pre-mature battery discharge in battery-powered devices.

This work was supported by C-BRIC, one of six centers in JUMP, a Semiconductor Research Corporation (SRC) program, sponsored by DARPA.

To realize adversarial sparsity attacks, we propose systematic methodologies that extend the principles of conventional adversarial attacks to identify the required input perturbations for any given DNN and input. We consider both white-box and black-box attack scenarios, which differ in the extent of the attacker’s knowledge of the DNN model. In a white-box scenario, where the attacker has full access to the model parameters, we define an objective function that measures the activation sparsity for a given input. We then utilize gradient-descent-based techniques to identify the required distortions that shift the input in the direction of decreasing the sparsity objective function. In black-box scenarios wherein model information is unavailable to the attacker, we demonstrate transferability of sparsity-attacked inputs. Further, in both cases, the attack is designed to be inconspicuous and cannot be detected by mere inspection of the DNN’s functional input and output. The end result is a very similar input that has no net functional effect on the classification, but incurs significantly reduced sparsity within the DNN and hence, increased classification time and energy.

We analyze the effectiveness of the attack by studying its performance under common defense techniques including input quantization and activation thresholding that intend to counter the attack’s impact by increasing activation sparsity. We find that these defenses are unable to recover the reduction in activation sparsity without sacrificing the accuracy of the network. This underscores the strength of the attack and also the need for future research efforts in developing specialized defense techniques. Finally, we also study the impact of the attack on different sparsity-optimized DNN platforms, including an accelerator and a general-purpose processor.

In summary, the key contributions of this work are:

- We introduce adversarial sparsity attacks, a new class of attacks that affect the latency and energy consumption of DNNs on sparsity-optimized platforms by reducing the amount of sparsity present in them.
- We propose systematic methodologies to introduce adversarial perturbations to DNN inputs in a manner that causes a decrease in activation sparsity without impacting classification accuracy in both white-box and black-box scenarios.
- We launch the attack on a set of 4 DNNs across 3 different datasets (MNIST, CIFAR-10 and ImageNet), and demonstrate a $1.16\times$ - $1.82\times$ decrease in activation sparsity with no loss in accuracy, for both white and black box attacks. We also demonstrate $1.12\times$ - $1.59\times$ and $1.18\times$ - $1.71\times$ increase in execution time and energy-delay product on a sparsity-optimized DNN accelerator.
- We investigate the effectiveness of three different defense techniques and demonstrate that the attack is largely impervious to these defenses, highlighting the need for further efforts towards specialized defenses.

The rest of the paper is organized as follows. Section II provides the necessary background on sparsity in DNNs as well as conventional adversarial attacks. Section III describes sparsity attacks and the proposed attack generation framework, and

Section IV discusses the defense techniques. The experimental methodology used to evaluate sparsity attacks is described in Section V. Section VI presents the results of applying sparsity attacks to DNN benchmarks. Finally, Section VII concludes the paper.

II. BACKGROUND AND RELATED WORK

This section describes the different types of sparsity in DNNs and their sources. It also presents some basic principles of conventional adversarial attacks, which are utilized in the proposed sparsity attack framework.

A. Sparsity in DNNs

Sparsity refers to the presence of zero-valued elements in different DNN data structures like weights and activations. Sparsity helps reduce the model size of DNNs and their overall memory requirements through the use of compact sparse storage formats. In addition, it also renders a large number of multiply-and-accumulate operations on zero-valued operands redundant, and skipping them helps reduce time and energy consumption in DNN implementations [5]–[10].

Sparsity in DNNs can be broadly classified into two categories:

- **Static Sparsity:** In static sparsity, the number and locations of zero values remain constant across different inputs to the network. Static sparsity arises in the static network parameters, *viz.* weights, and is typically introduced through pruning techniques [4].
- **Dynamic Sparsity:** In dynamic sparsity, the number and locations of zero values vary across different inputs to the network. Sparsity in activations is the primary example of dynamic sparsity and is caused by the presence of ReLU (Rectified Linear Unit) layers in the network, which zero out all negative values. State-of-the-art DNNs are known to contain significant dynamic sparsity. For example, activation sparsity varies from 40-70% across the DNNs we have considered in our experiments.

Figure 2 illustrates the variation in dynamic sparsity across a set of 500 images from Cifar10-Conv2, a network trained on Cifar-10 [14], with the architecture listed in Figure 8. We observe a variation of nearly $1.4\times$ across the different images. The degree of sparsity in a DNN determines its execution time and energy

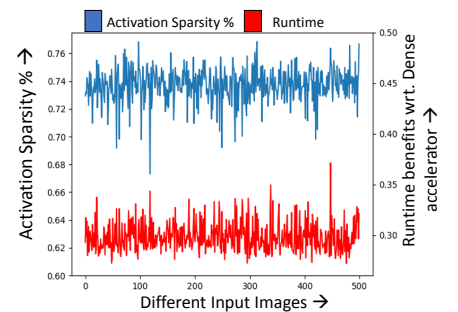


Fig. 2: Variation in input activation sparsity and execution time benefits across 500 images for Cifar10-Conv2 on Cnvlutin

accelerator

consumption on sparsity-optimized platforms [5]–[11]. Thus, the execution time of Cifar10-Conv2 varies by $1.38\times$ for the same 500 images on the Cnvlutin accelerator platform [6]. Our proposal of adversarial sparsity attacks exploits this property to modify inputs to a DNN in a manner that reduces the amount of dynamic sparsity, thereby negatively affecting its execution time and energy consumption on sparsity-optimized platforms.

B. Adversarial Attacks on DNNs

Adversarial attacks [15] have exposed serious security vulnerabilities in DNNs, raising a concern with their deployment in safety-critical applications like autonomous cars, unmanned aerial vehicles and healthcare. To date, adversarial attacks have focused on causing a neural network to misclassify an input by introducing small perturbations (typically imperceptible to human eyes).

Adversarial attacks can be classified as *untargeted* or *targeted*, depending on whether the aim of the attack is to generally degrade classification accuracy or to misclassify the input as a specific incorrect class. These attacks can also further be classified depending on the extent of information available to the attacker about the DNN model. White-box attacks assume that the attacker has complete knowledge of the network structure and parameters in addition to the class labels, whereas in black-box attacks the attacker is only aware of the class labels and/or confidence scores, but not the network structure and parameters. In many deployed systems, the fact that a DNN is used for classification, the network structure, or the entire model including weights are made public (*e.g.*, DeepFace from Facebook [16] and GPT3 from OpenAI [17]).

White-box attacks such as C&W[18] and MIM[19] calculate the gradients of the classification loss function with respect to the input. This gradient information is used to compute the necessary input perturbations that increase the probability of mis-classification. Black-box attacks, in contrast, are oblivious to the model parameters, and typically only assume access to the model’s output confidence scores for a given input. This renders the critical gradient information unavailable. Popular black-box attack strategies usually overcome this difficulty by approximately estimating the gradients [20] or the required perturbation directions [21]. For example, ZOO [20] estimates the gradient of the classification probabilities at a particular point in the input space by querying the user model repeatedly to obtain the classification scores at several closely spaced input points. The gradient is constructed by calculating the change in the output classification scores observed for the very small changes in the input values around the desired point. Other common black-box strategies take advantage of the transferable nature of the adversarial inputs [22].

Complementary to prior adversarial attacks, which aim to impact the DNN’s accuracy, our proposed class of attacks, *viz.* adversarial sparsity attacks instead affect the computational efficiency of DNNs.

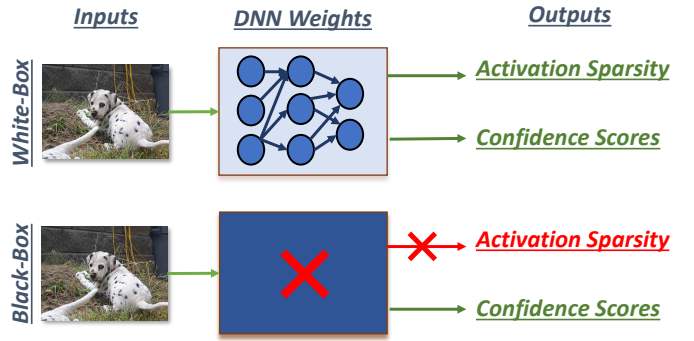


Fig. 3: Adversarial Sparsity Attacks in White and Black Box Settings

C. Timing Side Channel Attacks

The objective of timing side channel attacks, proposed in [23], is to more effectively launch accuracy-based adversarial attacks or membership inference attacks [24] in a black-box setting. The attack utilizes the execution time of a network to infer parameters like network depth. Using this information, the attacker constructs a new network that can better mimic the functionality of the unknown model, allowing it to launch a stronger attack. However, the attack does not target or affect the computational efficiency of the model on a hardware platform and is thus orthogonal to the adversarial sparsity attacks proposed in our work.

The following sections describe the details of adversarial sparsity attacks.

III. ADVERSARIAL SPARSITY ATTACKS

Adversarial sparsity attacks are a new class of attacks that perturb DNN inputs so as to decrease the sparsity of activation values, with the eventual goal of increasing DNN execution time and energy on sparsity-optimized platforms. This section presents an overview of these attacks and details the proposed attack generation framework.

A. Threat Models

In adversarial sparsity attacks, the intent of the attacker is to induce high classification time and energy consumption through carefully crafted input perturbations. For a pronounced impact on the user system’s battery life and classification latency, the attack needs to be persistent, *i.e.*, launched on several inputs over a long period of time. To facilitate this, the attack must evade trivial detection mechanisms such as observing the input and functional output of a DNN for anomalies. Specifically, the attack minimizes its impact on the input by adding perturbations that are bounded within a specified L_p limit, so that the resultant adversarial input is similar to the unperturbed input. In addition, the attack should ensure that the classification label assigned to an adversarial input is identical to that predicted by the network on the original input and consequently, the functional output of the DNN remains unchanged. In other words, the attacker

must craft an adversarial sample that is assigned the same label, regardless of the correctness of the original classification. Overall, the criteria for a successful sparsity attack can be summarized as:

- 1) The added perturbation must cause a significant reduction in activation sparsity
- 2) To prevent detection of the attack by observing the output, the classification prediction must be the same as that of the unperturbed input
- 3) To prevent detection of the attack by visual inspection of the input, the added distortions to the input must be imperceptible, i.e., within a specified L_p bound

Criterion 3 can be relaxed in scenarios wherein there is no supervision of the input image, such as autonomous navigation [25]. In such scenarios, the only feedback available to the user is the credibility or accuracy of the navigation - an aspect taken care of by satisfying Criterion 2. With the above criteria for a successful attack in place, we now discuss different attack scenarios that place varying constraints on the attacker's knowledge of the user model.

Figure 3 illustrates white-box and black-box scenarios for sparsity attacks. The attacker in a white-box scenario has full access to the user model's parameters such as the weights, and can consequently determine the internal activations. The attacker can thus calculate the overall activation sparsity for a given input, as well as its classification performance. In contrast, the attacker in a black-box scenario cannot access the model's internals, including weights and activations. Similar to state-of-the-art black-box attacks [20], [21] we assume that the attacker can query an input to obtain the output confidence scores. However, the attacker is prevented from evaluating the overall activation sparsity for a given input.

B. Attack Strategies

We will now elucidate the attack strategies developed to realize sparsity attacks in both white-box and black-box scenarios.

1) White-Box Sparsity Attacks: The proposed white-box attack uses a composite objective function that combines the overall activation sparsity with the classification loss of the network for a given input. Next, it calculates the gradient of this objective function with respect to the input to reveal the relationship between changes in the input and the corresponding effect on the activation sparsity and classification loss. Finally, by incorporating these gradients into iterative gradient-descent techniques, the attacker obtains the necessary perturbations that decrease activation sparsity while minimizing the classification loss.

The objective function, \mathcal{L} , that combines the overall activation sparsity and classification loss for a given input can be described by Equation 1.

$$\mathcal{L}(x) = \mathcal{L}_{sparsity}(x) + c \cdot \mathcal{L}_{ce}(x) \quad (1)$$

Algorithm 1 Creating inputs for adversarial sparsity attacks

Input: x_{clean} (Clean Input), f (DNN model), $\mathcal{L}_{sparsity}$ and \mathcal{L}_{ce} (Objective function terms), ϵ (Maximum L_2 distortion), ϵ_{iter} (L_2 distortion per iteration), O_{max} and I_{max} (Maximum outer and inner-loop iterations), c_{in} , c_{min} and c_{max} (Initial, min. and max. value of trade-off constant)

Output: x_{adv} (Adversarial input)

```

 $c = c_{in}, o = 1$ 
while  $o < O_{max}$ 
   $x_0 = x_{clean}, i = 1, g_0 = 0$ 
  while  $i < I_{max}$ 
     $\mathcal{L}(x_i) = \mathcal{L}_{sparsity}(x_i) + c \cdot \mathcal{L}_{ce}(x_i)$ 
     $g_i = \mu g_{i-1} + \nabla_x \mathcal{L}(x_i)$ 
     $x_{i+1} = x_i - \epsilon_{iter} \cdot \frac{g_i}{\|g_i\|_2}$ 
     $x_{i+1} = Clip_{[0,1,\epsilon,x_{clean}]}(x_{i+1})$ 
     $i = i + 1$ 
  if  $argmax(f(x_{adv})) \neq argmax(f(x_{clean}))$ 
     $c = (c + c_{max})/2$ 
  else
     $c = (c + c_{min})/2$ 
   $o = o + 1$ 

```

where c is the Lagrange multiplier or the trade-off constant, $\mathcal{L}_{sparsity}$ estimates the overall activation sparsity across the network for an input x , \mathcal{L}_{ce} measures the classification cross-entropy loss of the input x with respect to the *target class assigned by the network on the original unperturbed input*. We note here that \mathcal{L}_{ce} is not calculated against the ground-truth labels, since our objective is to mimic the DNN's behavior on unperturbed inputs.

The intent of the attacker is to calculate input perturbations that minimize the measure of the objective function \mathcal{L} , i.e., cause a reduction in activation sparsity and specified classification loss. The gradient of \mathcal{L} with respect to the input image is thus used to calculate the required perturbations that push the input in the direction of decreasing activation sparsity, while maintaining the same classification accuracy, i.e., keeping the predicted labels to be identical to that of the original input. Intuitively, the choice of the trade-off constant c impacts the performance of the sparsity attack - it is important to choose a value of c that achieves a high degradation in activation sparsity without sacrificing accuracy. Further, it must also be ensured that the added perturbations are within the maximum L_2 distortion allowed, i.e., Criterion 3. The entire process that addresses these aspects is outlined in Algorithm 1.

The functioning of Algorithm 1 can be explained in two parts. First, for a particular value of the trade-off constant c , the algorithm uses gradient-descent techniques (Lines 4-9) to calculate the perturbations (L_2 bounded) that decrease activation sparsity while maintaining similar classification predictions. Next, to maximize the performance further, the algorithm employs simple binary-search techniques that identify an optimal c (Lines 10-14).

Focusing on the gradient-descent process first, we begin by initializing the perturbed input x_0 to the original input x_{clean}

(line 3). In every iteration i , the gradient of $\mathcal{L}(x_i)$ with respect to the input is evaluated at x_i (line 5). There are several gradient-descent based optimization algorithms that can be incorporated to update the input. In our experiments, we find that utilizing standard gradient descent with a momentum-based update [26] typically provides the best results, as shown in line 6. The momentum parameter μ is set to 0.9 in all our experiments. Using the gradient values, a small distortion is calculated so as to push x_i in the direction of decreasing sparsity and classification loss (line 7). Finally, at the end of the iteration i , the perturbed input is clipped so as to ensure the added distortions are within the L_2 bound ϵ , and does not exceed the permissible input value range i.e., $[0, 1]$ (line 8). This process is continued for I_{max} iterations.

At the end of I_{max} iterations, the binary search process for finding an optimal c comes into play. As can be seen, the classification prediction of the perturbed input is first evaluated and compared against the prediction on the original input (line 10) - if the labels do not match, the priority of the \mathcal{L}_{ce} term is increased by increasing c as indicated in line 11. On the contrary, if the labels do match, this indicates that the attacker can afford to assign the $\mathcal{L}_{sparsity}$ term a higher priority, by decreasing c (line 13). Starting the next outer-loop iteration the perturbation and gradient variables are reset (line 3), and the process is continued until O_{max} iterations are complete. The output of the algorithm is an adversarially perturbed input x_{adv} that successfully decreases the activation sparsity of the user system, while satisfying Criterion 2 and 3 as well.

Naturally, the convergence and the resulting performance of Algorithm 1 is contingent on the specific forms of the \mathcal{L}_{ce} and $\mathcal{L}_{sparsity}$ functions. We will now describe the process of suitably designing these objective function terms that play a crucial role in determining the efficacy of the adversarial sparsity attack.

Design of $\mathcal{L}_{sparsity}$: For successfully satisfying Criterion 1, the function representing $\mathcal{L}_{sparsity}$ must effectively quantify the overall activation sparsity across the network for a given input. Ideally, we could apply a step function on the input activations of every layer in the network to determine whether it is non-zero, and perform a summation of the resulting step-function outputs across the network to determine the total activation sparsity. However, the objective function must also be differentiable in the input activation range so that the gradients can be calculated in Line 6 of Algorithm 1. To that end, we devise continuous versions of the step function to detect non-zero activation values in the network.

We specifically use Tanh and Sigmoid functions, described by the following equations, in our framework:

$$\text{Tanh}(\beta, act) = \frac{e^{\beta \cdot act} - e^{-\beta \cdot act}}{e^{\beta \cdot act} + e^{-\beta \cdot act}} \quad (2)$$

$$\text{Sigmoid}(\beta, act) = \frac{1}{e^{-\beta \cdot act} + 1} \quad (3)$$

where act is an input activation to a layer in the network. Both the functions are differentiable, and the value of β can be

increased to improve their resemblance to the step function. An estimate of the number of non-zero neurons across all the layers of the network is obtained by summing the individual input activations with the tanh or sigmoid functions applied on top of them. We define such an estimate E as:

$$E(x) = \sum_L \sum_{N_l} F(I(n_{l,x})) \quad (4)$$

where F refers to the sigmoid or tanh function and $I(n_{l,x})$ refers to the n^{th} input activation of layer l for a given input, x . To estimate the overall degree of zero-valued neurons, E must be negated before application in Algorithm 1. We further normalize E to the total number of neurons in the network. The final $\mathcal{L}_{sparsity}$ can thus be expressed as:

$$\mathcal{L}_{sparsity}(x) = -\frac{E(x)}{k} \quad (5)$$

where k refers to the network's total neuron count.

Figure 4 illustrates the efficacy of the sparsity attack on Cifar10-Conv2, using tanh and sigmoid objective functions with varying β . As can be seen for both the tanh and sigmoid functions, the decrease in activation sparsity obtained by the attack improves with increasing β until saturation is reached at some point. Across all networks, for a particular value of β , we observe that the tanh function tends to perform better than the sigmoid function by decreasing the final activation sparsity by an additional 8% on an average. We report the β values to be used in conjunction with the tanh function for the best results on the networks considered in our experiments in Section V.

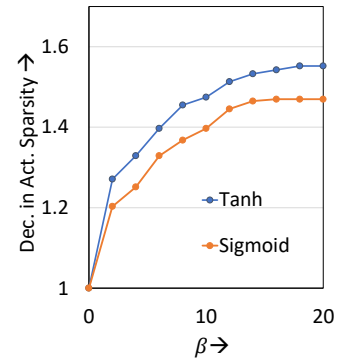


Fig. 4: Impact of β on decrease in activation sparsity

To ensure a higher impact of reduced sparsity on the execution time and energy consumption of different sparsity-optimized platforms, we also augment the objective function $\mathcal{L}_{sparsity}$ with some hardware-specific parameters. We specifically weigh the sparsity terms corresponding to each layer with values proportional to their relative execution time and energy consumption on a given hardware platform. In other words, time and energy intensive layers are assigned higher weight values in the overall objective function. The modified sparsity estimator function E can thus be described by the following equation.

$$E(x) = \sum_L W_l \sum_{N_l} F(I(n_{l,x})) \quad (6)$$

where W_l is the weight assigned to layer l and is set to be equal to the relative runtime or energy consumption of that layer on the considered hardware platform.

Design of \mathcal{L}_{ce} : As per Criterion 2, the classification label predicted by the network on the perturbed input must match

the label assigned by the network on the unperturbed input. Accordingly, \mathcal{L}_{ce} must measure the classification loss of the input with respect to the original predicted label. Akin to the design of objective functions for targeted attacks [19], we define \mathcal{L}_{ce} as the softmax cross-entropy loss with respect to the ‘target’ label y . For original and adversarial inputs x_{clean} and x_{adv} this can be expressed as:

$$y = \operatorname{argmax}(f(x_{clean})) \quad (7)$$

$$\mathcal{L}_{ce}(x_{adv}) = -\log\left(\frac{e^{f(x_{adv})_y}}{\sum_{l=1}^N e^{f(x_{adv})_l}}\right) \quad (8)$$

where $f(x)$ is the pre-softmax output of the DNN for input x , y is the class label assigned by the network on the original input x_{clean} , N is the number of classes and $f(x)_l$ is the pre-softmax output with respect to class l .

In summary, white-box sparsity attacks exploit their knowledge of the model parameters by utilizing iterative gradient-descent based techniques to find the required perturbations that satisfy Criteria 1-3.

2) *Black-Box Sparsity Attacks*: In this subsection, we describe strategies to launch a sparsity attack in a black-box scenario.

As shown in Figure 3, the attacker in a black-box scenario can access only the classification performance of the network and is unaware of the network weights, activations, and consequently, the overall sparsity. This precludes the attacker from directly utilizing the gradient-descent-based attack methodology described in Algorithm 1. As mentioned in Section II, conventional state-of-the-art black-box attacks work around this challenge by iteratively determining approximations of either the gradient of the classification performance [20], or the appropriate direction of perturbation [21]. These approximations solely require the classification confidence scores for a given input, and do not require any knowledge of the network weights. Unfortunately, we cannot adopt similar techniques in black-box sparsity attacks as the amount of sparsity in a network cannot be estimated from the queried classification scores of the user model. Hence, we explore alternative techniques for launching a black-box sparsity attack.

First, we investigate whether adversarial sparsity attack inputs are *transferable* between different networks, *i.e.*, whether an adversarial input generated for a known substitute (or surrogate) model [22] using the white-box technique can have the desired effects on the unknown user model. To evaluate such transferability, we first perform the white-box attack described in the previous subsection on Cifar10-Conv2 (the substitute model, and whose architecture is listed in Section V), and subsequently transfer the images to 3 different Cifar10 models whose architectures are listed for reference in Figure 5, but assumed to be unknown to the attacker.

On deploying the white-box attack on Cifar10-Conv2, the average decrease in activation sparsity across the test dataset is $1.56\times$, for no loss in classification accuracy. In Figure 6 we depict the decrease in activation sparsity and classification

Model	Architecture
Model 1	Conv(3*3*32), ReLU, (2*2 Max Pool), Conv(3*3*32), ReLU, (2*2 Max Pool), Conv(3*3*64), ReLU, Conv(3*3*64), ReLU, FC(512), ReLU, FC(10), Softmax
Model 2	Conv(5*5*64), ReLU, (3*3 Max Pool), Conv(5*5*64), ReLU, (3*3 Max Pool), Conv(3*3*64), ReLU, Conv(3*3*32), ReLU, FC(512), ReLU, FC(10), Softmax
Model 3	Conv(3*3*32), ReLU, (2*2 Max Pool), Conv(3*3*32), ReLU, Conv(3*3*32), ReLU, FC(64), ReLU, FC(10), Softmax

Fig. 5: Architecture of different unknown models

accuracy incurred by the unknown models when these images are passed through them. For the sake of comparison, we also illustrate the performance of the white-box sparsity attack on all three models. Across all unknown models, it is observed that the decrease in activation sparsity exhibited by simply transferring the images is only 10-12% lower than that obtained by the white-box attack on the same model. However, unfortunately, there is a significant decrease in classification accuracy - nearly 60%. Hence, while sparsity-attacked images appear to be transferable in terms of the reduction in activation sparsity,

classification accuracy is clearly not maintained. We find this to be inline with the results reported in several accuracy-based black-box attack research efforts such as [20], [27], which observe that unlike untargeted attacks, targeted attacks exhibit poor transferability, and require specialized techniques such as [20], [21], [27] for achieving high attack success rates.

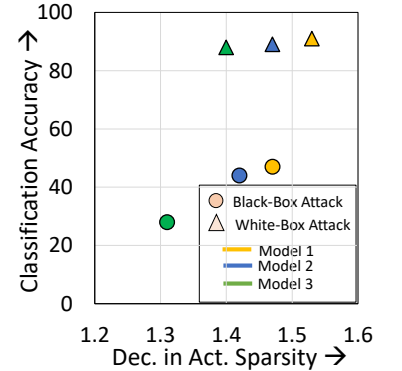


Fig. 6: Analyzing the transferability of the adversarial sparsity attack

To resolve the aforementioned challenges, we propose a two-stage framework that first derives attack inputs on a known substitute model, transfers those inputs to the unknown model only for the purpose of reducing sparsity and (if needed) finally applies an accuracy-based targeted black-box attack to restore the original prediction label. Figure 7 summarizes the overall black-box sparsity attack process. As shown in the Figure 7, the first stage generates adversarial sparsity images on a substitute model using the white-box attack mechanism of Algorithm 1, with c set to zero. In the second stage, to ensure that predictions are maintained, all mis-predicted images are passed through the ZOO targeted accuracy-based black-box attack[20]. ZOO repeatedly queries and observes the changes in classification performance for some closely-spaced input points to determine the gradients for a particular input and utilizes these gradients to find the necessary perturbations to change the network output to the targeted class. As in white-box sparsity attacks, the target class is the class predicted by the unknown network on the

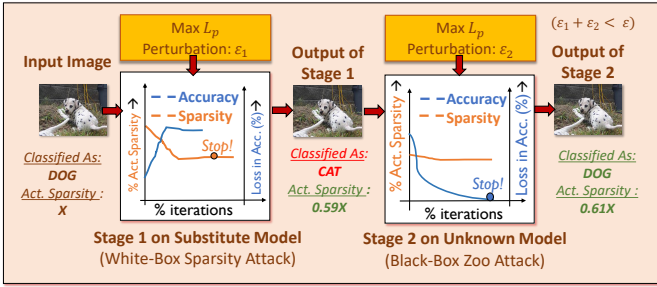


Fig. 7: Two Stages of the Black-Box Sparsity Attack

unperturbed input. Experimental results indicate that although the second stage does not factor activation sparsity, the impact on the decrease in activation sparsity achieved by the first stage is minimal i.e., *within 2%*, across the networks considered. We also place additional constraints to ensure that the total L_2 distortion introduced by both stages, ϵ_1 and ϵ_2 respectively, is within the specified limit ϵ .

In summary, our black-box sparsity attack is realized in two stages that first transfer adversarial sparsity attack inputs created on a substitute model and then apply targeted black-box attacks to restore the functional output if needed.

IV. POTENTIAL DEFENSE TECHNIQUES

In this section, we outline potential defense techniques against adversarial sparsity attacks and evaluate their efficacy. The defense techniques broadly aim to restore activation sparsity, thereby countering the impact of the sparsity attack. In the process, successful defenses should not negatively impact the classification accuracy of the DNN as well. It is further imperative that the chosen defense be computationally lightweight—it would be counter-productive if the defense itself added a significant latency or energy overhead in order to prevent the latency or energy increase incurred by the attack.

We specifically discuss the key principles of three different computationally light-weight defense techniques below.

A. Activation Thresholding

Activation thresholding, as the name suggests, involves setting all activations below a certain non-zero threshold to zero, thereby increasing the overall activation sparsity. The thresholds must be set to values that cause no loss in accuracy on unperturbed inputs. Further, the threshold values can be identified at a per-layer granularity. In our implementation, we initialize the threshold of each layer to the mean activation value of that layer as measured on the adversarial set, and iteratively increase or decrease its value till an increase in activation sparsity is obtained for a tolerable loss in accuracy.

B. Adversarial Training

Adversarial training [28] is a popular defense technique used in classical accuracy-based adversarial attacks. It involves generating adversarial examples on the clean training set, and

then retraining the model with the original training examples augmented with the adversarially generated samples. Such techniques have shown great success at mitigating the impact of attacks like FGSM [29], PGD [30], *etc.*

Although adversarial training was formulated as a defense technique to mitigate accuracy-based attacks, we investigate its suitability for adversarial sparsity attacks. The aim of adversarial training in this context is to increase the activation sparsity of the adversarial inputs to match that of unperturbed input samples. We generate the inputs for adversarial training using the white-box techniques discussed in Section III, and the parameters listed in Section V.

C. Input Smoothing

Adversarial sparsity attack distortions are calculated perturbations added to the input so as to reduce activation sparsity while maintaining classification accuracy. We investigate whether the impact of the sparsity attack can be nullified by input smoothing techniques, namely input quantization and compression, similar to the techniques used in [31] to defend against conventional adversarial attacks. We select appropriate parameters for each smoothing technique such that they mitigate the impact of the sparsity attack while incurring no loss in accuracy. For example, we select the bit-width or compression quality which provide the best defense against the attack. Our formula for k -bit input quantization applied on an input x is expressed as:

$$x_q = \frac{1}{2^k} \cdot \text{round}((2^k) \cdot x) \quad (9)$$

Input compression applies to images, and as the name suggests, consists of applying image compression to the image to remove high-frequency artifacts. To realize input compression with quality k , we pass the input image x to the `encode_jpeg` method from TensorFlow [32] with quality set to k .

For all of the above defenses, we assume that the attacker does not adapt to the defense technique. However, as we will be demonstrating in Section VI, none of the defenses explored here show significant mitigation of the sparsity attack - to reduce the impact of the sparsity attack by even 8% (in activation sparsity) on the adversarial set, a 4% loss in unperturbed accuracy must be incurred, which is an unacceptable tradeoff in most practical scenarios. This emphasizes the strength of the sparsity attack to withstand conventional defenses. We do not consider other popular techniques such as GANs [33] or variational auto-encoders [34] used in accuracy-based attacks as they incur significant computational overheads themselves. Nevertheless, this may be an interesting direction to investigate as part of future efforts.

A possible *detection* mechanism involves measuring the latency or the energy consumption of the hardware system. If the energy consumption goes beyond a certain range, the user could be alerted. We note however that while this aids in detection of the attack, it does not resolve or counter the impact of the attack. Further research is needed to produce a successful defense technique, which will be explored as in future work.

V. EXPERIMENTAL METHODOLOGY

Datasets and Model Architectures. We demonstrate the effectiveness of adversarial sparsity attacks on 4 different image-recognition DNNs across 3 different datasets (MNIST [35], CIFAR-10 [14] and ImageNet [36]). The details of the architectures are listed in Figure 8. The ImageNet-Conv and Cifar10-Conv2 architectures are taken from [12], [37]. The white-box and black-box attacks are conducted on the full test set, except in the case of the black-box attack launched on ImageNet-Conv wherein we report results for 1000 randomly selected test set images. The reduction in activation sparsity inflicted by the attack does not vary significantly across images (<5%). We report the average reduction in activation sparsity, and the corresponding increase in classification latency and energy-delay product for each network in Section VI.

Dataset	Name	#Layers		Architecture	Acc %
		Conv	FC		
MNIST	Mnist-Conv	4	2	Conv(3*3*20), ReLU, Conv(3*3*20), ReLU, (2*2 Max Pool), Conv(3*3*20), ReLU, Conv(3*3*20), ReLU, FC(500), ReLU, FC(10), Softmax	99.45
CIFAR 10	Cifar10-Conv1	4	2	Conv(3*3*32), ReLU, Conv(3*3*32), ReLU, (2*2 Max Pool), Conv(3*3*64), ReLU, Conv(3*3*64), ReLU, (2*2 Max Pool), FC(512), ReLU, FC(10), Softmax	89.6
	Cifar10-Conv2	9	-	AllConvNet	90.9
ImageNet	ImageNet-Conv	13	3	VGG16	71.3

Fig. 8: Employed model architectures

The attack framework is implemented using TensorFlow [32]. We utilize the software framework provided in [20] to realize the second stage of the black-box attack. The different hyper-parameters used by white-box and black-box attacks are listed in Figures 9(a) and 9(b), respectively. Additionally, for the white-box attack, we set O_{max} to 1, and c_{in} , c_{min} and c_{max} to 0.5, 0 and 1, respectively, in all our experiments. The optimality of these hyper-parameters is discussed in Section VI-A. The first stage of the black-box attack is conducted using the same parameters listed in Figure 9(a). The substitute models used in this step are discussed in Section VI-B.

Parameter	MNIST -Conv	Cifar10 -Conv1	Cifar10 -Conv2	ImageNet -Conv	Parameter	Value
$\epsilon_{iter}(L_2)$	0.02	0.01	0.01	0.01	Binary Search Steps	1
$\epsilon(L_2)$	0.9	0.9	0.9	0.8	Initial Constant	0.5
I_{max}	75	100	100	100	Number of iterations	10000
β	15	16	20	22	Learning rate	0.002

(a)

(b)

Fig. 9: Hyper-parameter values used for a) White-Box sparsity attack and b) Stage 2 of the Black-Box sparsity attack

Sparsity-optimized platforms. We evaluated the effects of adversarial sparsity attacks on two different sparsity-optimized platforms, namely, the Cnvlutin DNN accelerator [6] and the SPARCE general-purpose processor [8]. The micro-architectural details of each of these platforms are listed in Figure 10.

For measuring execution times on Cnvlutin, we develop a cycle-accurate simulator using the details provided in [6]. Our developed simulator closely matches the execution time and energy consumption values reported in [6] for a given network. We utilize a simulator provided to us by the authors of SPARCE for measuring execution times and energy consumption. For both platforms, the execution time and energy consumption is obtained for the unperturbed and adversarial inputs.

Parameter	Value	Parameter	Value
Frequency	1 GHz	Processor Config.	ARMv8-A, In-order
Area	70 mm ²	SPARCE Config.	20 SASA table entries, 32 SpRF entries
Size	65 nm	L1 Cache	Split I&D, 32KB I cache, 64KB D cache
Num. Of PEs	16	L2 Cache	Unified 2MB

(a)

(b)

Fig. 10: Micro-architectural details for a) Cnvlutin and b) SPARCE

VI. RESULTS

In this section, we present the results of our experiments demonstrating the effectiveness of the proposed adversarial sparsity attacks.

A. White-Box Sparsity Attacks

1) Impact on Activation Sparsity, Execution time and EDP: We first evaluate the decrease in activation sparsity, and corresponding increases in execution time and energy-delay product, resulting from white-box adversarial sparsity attacks.

Decrease in Activation Sparsity: The decrease in activation sparsity achieved by the white-box sparsity attack under two different perturbation constraints is shown in Figure 11. In certain scenarios where human supervision of both the input and output of the DNN is present, it is necessary that the sparsity attack meets all criteria listed in Section III. Specifically, the added input distortions should be imperceptible, i.e., constrained within the L_2 bound specified in Figure 9. We refer to these attack scenarios as constrained. However, in scenarios such as autonomous self-driving where there is no human supervision of the input, this criterion can be relaxed, i.e., the added perturbations can be of any magnitude provided the pixel values are within a valid range i.e., [0,1]. The only behavior observable to the user in such scenarios is the correctness of the classification. This is considered by the attack through Criterion 2, i.e., no change in classification output. Such an attack scenario is referred to as unconstrained, wherein it is sufficient to satisfy just Criteria 1 and 2. Across the networks considered the proposed white-box sparsity attack achieves a $1.16 \times - 1.52 \times$ (average: $1.26 \times$) decrease in activation sparsity for the constrained case. These values increase to $1.55 \times - 1.82 \times$ (average: $1.71 \times$) for the unconstrained scenario.

As the activation sparsity of the networks considered vary from 50%-70%, a trivial limit for the maximum reduction in sparsity

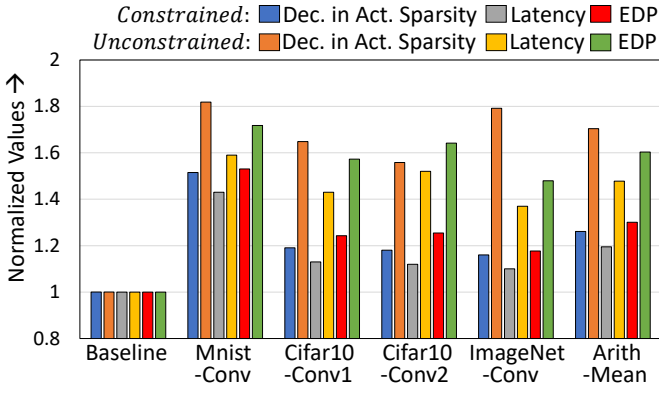


Fig. 11: Impact of white-box adversarial sparsity attacks on activation sparsity, execution time and EDP on Cnvlutin

possible would range from $2\times-3\times$, i.e., bringing activation sparsity down to 0. Such extremely low sparsity levels may be hard to attain while maintaining accuracy. A more meaningful and tight limit is difficult to establish because at the heart of the attack lies a non-convex optimization problem with upto tens of thousands of variables (corresponding to the input size).

The reduction in sparsity achieved by the attack translates to varying degrees of execution time and energy increase depending on the DNN, as discussed next.

Increase in Execution Time: Figure 11 also shows the impact of adversarial sparsity attacks on the execution time of different networks on the Cnvlutin [6] accelerator. We observe a slowdown of $1.12\times-1.43\times$ (average: $1.20\times$) across all networks for the constrained scenario, which increases to $1.37\times-1.59\times$ (average: $1.49\times$) for the unconstrained case. Comparing results across datasets, we note that for some datasets, sparsity may be present in the input image itself, allowing the sparsity attack to also target the first layer of the network in addition to the subsequent layers. Specifically, the images in the MNIST dataset are sparse ($\sim 80\%$), while the CIFAR-10 and ImageNet datasets exhibit minimal (0-0.3%) sparsity in the input. Thus, for the CIFAR-10 and ImageNet networks, decreases in sparsity and the corresponding impact on execution time and energy are possible only from the second convolutional layer onwards. As a result, networks with comparatively smaller runtimes for the first convolutional layer, such as Cifar10-Conv2 and ImageNet-Conv feel the impact of decreased sparsity in a more pronounced fashion unlike networks such as Cifar10-Conv1, whose first convolutional layer alone nearly takes up 26% of the total runtime.

Increase in EDP: We utilize Energy-Delay Product (EDP) as a metric to evaluate the effect of adversarial sparsity attacks on energy efficiency of DNN execution. Sparsity attacks cause an increase in energy consumption due to the higher number of operations to be performed. This results in a $1.18\times-1.53\times$ (average: $1.30\times$) increase in EDP for Cnvlutin when the perturbations are constrained. When the constraints are relaxed, the increase in EDP ranges from $1.47\times-1.71\times$ (average: $1.6\times$).

2) *Impact on the activation sparsity distribution:* We

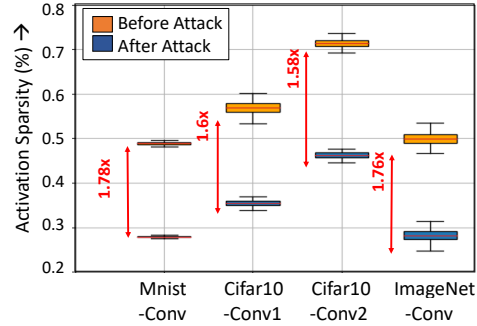


Fig. 12: Distribution of activation sparsity before and after application of the attack

observe the change in the activation sparsity distribution across the test dataset images as a result of the sparsity attack. Figure 12 depicts a box-whisker plot of the activation sparsity distribution on all networks, before and after the application of the sparsity attack. As marked by the red arrows, the worst case sparsity of the adversarial inputs is $1.58\times-1.78\times$ lower than the worst case sparsity of the clean inputs. Clearly, even if designers account for the worst case sparsity present in the clean inputs, the attack reduces sparsity further by a significant degree, causing inference time and energy to exceed the limits of even a conservative design.

Additionally, we also provide a visualization of the distribution of values at the output of a convolutional layer prior to the application of the ReLU activation. In Figure 13 we depict the pre-ReLU activations at the output of the first convolutional layer of Cifar10-Conv2 before and after the attack has been launched. As indicated by the median values of the clean and adversarial samples, under the influence of the attack the

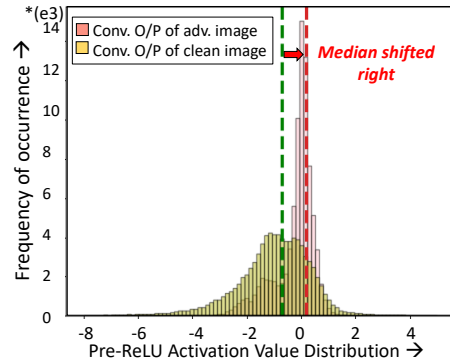


Fig. 13: Distribution of activation values at the output of the first convolutional layer of Cifar10-Conv2

negative pre-ReLU activations are shifted towards the right, i.e., the activation value distribution becomes more positive. This leads to a decrease in post-ReLU activation sparsity. However, note that the pre-ReLU activations are limited to values of small magnitude, which helps in preserving the network output, and hence, accuracy.

3) *Analyzing impact of different hyper-parameters:*

Impact of c : We now analyze the performance of Algorithm 1 in terms of the hyper-parameter c , i.e., the trade-off space between achieving a significant decrease in activation sparsity while incurring no loss in classification accuracy. At $c = 0$, Algorithm 1 solely focuses on reducing the activation sparsity of the network, and does not factor classification performance. On Mnist-Conv, this point translates to nearly $1.85\times$ decrease in activation sparsity on average across images, but a 70%

decrease in classification performance. Interestingly, Algorithm 1 identifies a higher value at $c = 0.3$, at which there is absolutely *no loss in classification accuracy* and $1.83\times$ decrease in activation sparsity - merely 2% below the reduction in activation sparsity obtained at $c = 0$. These results indicate the ability of the algorithm to identify points on the objective landscape that ensure virtually no impact on classification accuracy, whilst only marginally compromising on the decrease in activation sparsity.

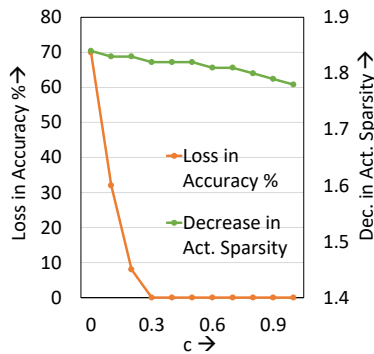


Fig. 14: Impact of c on performance of Algorithm 1

Impact of O_{max} and I_{max} : In Figure 14, the presence of a plateau-region in both the sparsity and accuracy curves for a wide range of c values indicates the low sensitivity of the performance of Algorithm 1 to c in this range - an insight that we exploit to drastically reduce the number of binary-search step iterations to find an optimal c . Across our networks, providing any c_{in} in the range of 0.5 to 1 achieves adequate results in merely 1 outer-loop iteration. This is further underscored in Figure 15, which depicts the minimal impact of increasing O_{max} on the performance of Algorithm 1 when $c_{min}=0.2$, $c_{in}=0.6$ and $c_{max}=1$, in the context of Cifar10-Conv2. Across all curves, for each outer-loop iteration

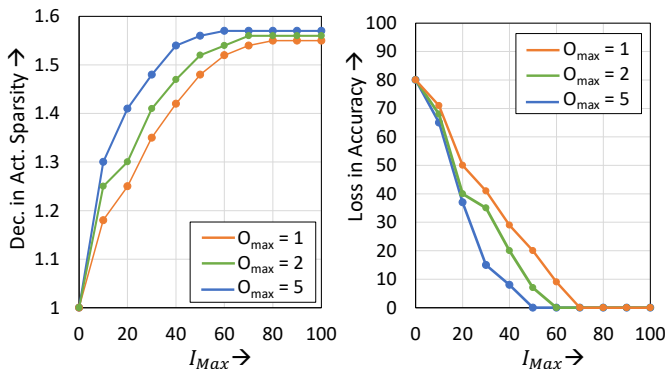


Fig. 15: Impact of O_{max} and I_{max} on performance of Algorithm 1

it typically takes around 40-50 inner-loop iterations for the accuracy to converge, and an additional 20-40 iterations for the decrease in activation sparsity to saturate, with higher O_{max} requiring slightly fewer inner-loop iterations. All values of O_{max} considered varying from 1 to 5 ensure correct predictions after the total $O_{max}\cdot I_{max}$ iterations have completed. More importantly, we observe that higher values of O_{max} , which engage in finding a better c than c_{in} only provide at most 2-3% improvement in the decrease in activation sparsity, over $O_{max} = 1$. Therefore, across our networks, we conduct our white-box attacks with O_{max} set to 1, ensuring a runtime-efficient attack with little to no sacrifice in performance.

4) *Runtime Analysis:* We list the runtimes involved in launching the white-box sparsity attack on each network in Figure 16, with all experiments conducted on a single NVIDIA-RTX2080Ti GPU. For reference, we also compare our runtimes against state-of-the-art accuracy-based attacks namely Projected Gradient Descent (PGD) [30] and Carlini and Wagner (C&W) [18] on the same networks, for an equal number of total iterations. As observed, the runtime costs of our attack are on average only marginally higher than PGD (by 18%), and faster than C&W (by 6%). This highlights the computational feasibility of the proposed adversarial sparsity attacks.

Attack Setting	Attack	MNIST-Conv	Cifar10-Conv1	Cifar10-Conv2	ImageNet-Conv
White Box	Sparsity Attack	0.14 min	0.18 min	0.41 min	20 min
	C&W	0.15 min	0.19 min	0.42 min	22 min
	PGD	0.11 min	0.16 min	0.34 min	18 min
Black Box	Sparsity Attack	1.84 min	4.2 min	5.24 min	78 min
	ZOO	1.7 min	4 min	4.8 min	57 min

Fig. 16: Runtimes per image for sparsity attacks and conventional accuracy-based attacks

B. Black-box attacks

1) Impact on Activation Sparsity, Execution Time and EDP:

We study the effect of black-box sparsity attacks on all networks for the unconstrained distortion scenario, and demonstrate the increase in execution time and EDP on the Cnvlutin accelerator. For the Cifar10 and MNIST networks, we use Model 1 described in Figure 5 as the substitute model, and employ the VGG-19 [12] architecture as the substitute when attacking the ImageNet network. The white-box sparsity attack causes a $1.53\times$ and $1.48\times$ sparsity reduction on Model 1 for the Cifar10 and MNIST datasets respectively, and a $1.65\times$ reduction in sparsity for the VGG-19 model. As shown in Figure 17, we achieve a $1.43\times - 1.67\times$ decrease in activation sparsity, which translates to $1.24\times - 1.5\times$ increase in execution time, and $1.35\times - 1.62\times$ increase in EDP. These results demonstrate that sparsity attacks can be effectively launched in black-box scenarios as well.

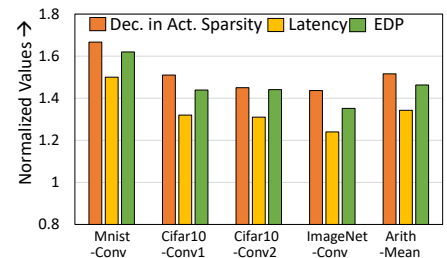


Fig. 17: Impact on Activation Sparsity, Latency and EDP for Black-Box attacks

2) *Impact of Substitute Model on Performance:* Figure 18 illustrates the impact of using different substitute models when launching a black-box attack on Cifar10-Conv1 and Cifar10-Conv2, with the models listed in Figure 5 used as substitute models. The effectiveness of the transfer is dictated

by two factors: a) the inherent vulnerability of the unknown network to the sparsity attack and b) the vulnerability of the substitute model deployed. Our experiments suggest that, the final reduction in sparsity achieved by the black-box attack is generally upper bounded by impact of the white-box attack on the same DNN. Moreover, in certain cases, if the

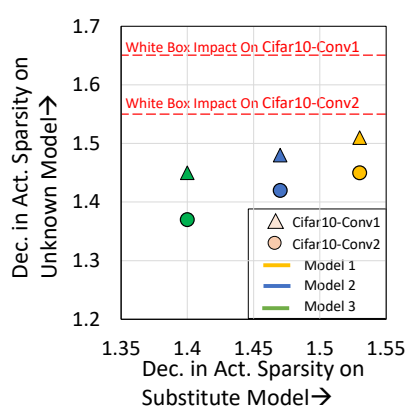


Fig. 18: Analyzing impact of Substitute Model

unknown model is highly susceptible to the attack, it can exhibit a higher reduction in sparsity than that incurred by the substitute model. This trend is observed when using Model 3 to attack Cifar10-Conv1. Further, amongst the different substitute models deployed, we empirically find that substitute models that exhibit higher vulnerability to the white-box attack are more likely to induce a transfer of higher potency.

3) *Runtime Analysis*: Figure 16 also lists the runtimes of black-box attacks across different networks. The higher runtime of the black-box sparsity attack compared to the white-box version is attributed to the second stage, which employs a targeted accuracy-based attack to ensure that the perturbed input does not cause a change in the DNN’s output. Such targeted black-box attacks have been reported to be significantly more expensive to compute than their white-box counterparts. This is due to the increased difficulty in estimating the gradients that are critical towards attaining high success rates. For example, conducting the black-box sparsity attack on Cifar10-Conv1 for example takes 4.2 min per image, which is far higher than the 0.18 min per image required for the white-box sparsity attack. Comparing the runtimes of black-box sparsity attacks against that of the ZOO attacks on the same networks, we find that our attack is on average merely 13% more expensive to compute, due to the relatively small overhead of the first stage.

C. Analysis of defense techniques

In this subsection, we study the effectiveness of the defense techniques discussed in Section IV against the white-box attacks, in the unconstrained distortion scenario. Figure 19(a) illustrates the trade-off between the loss in unperturbed accuracy and the decrease in activation sparsity for the activation thresholding defense. We report results for four configurations that attempt to restore sparsity while incurring within 0%, 1%, 2% and 5% drop in unperturbed accuracy, respectively. The configurations that provide no loss in accuracy have negligible effect on the impact of the attack. Further, even with a 5% loss in accuracy, the defense is only able to degrade the attack’s impact on sparsity by 6-8% across networks.

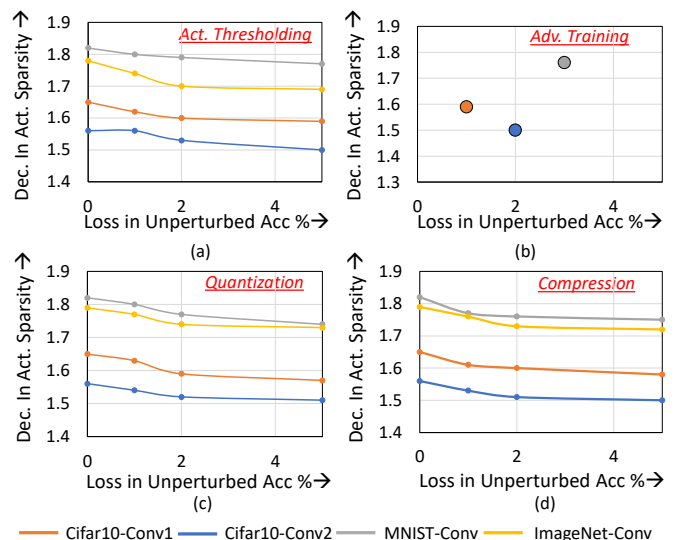


Fig. 19: Analyzing the impact of different defense techniques

The results for input quantization [Figure 19(c)] and compression [Figure 19(d)] tell a similar story. On Cifar10-Conv2 an input bit-width of 4, or a compression quality of 75 (out of 100) mitigates the attack’s impact by 5-6%, whilst incurring a 5% drop in unperturbed accuracy. It is evident that, to mitigate the impact of sparsity attacks considerably, the defender must resort to using extremely low precision bitwidths and compression qualities for the input, which generally cause a severe reduction in unperturbed accuracy. We report similar findings for adversarial training, as seen in Figure 19(b).

D. Evaluation on general-purpose processors

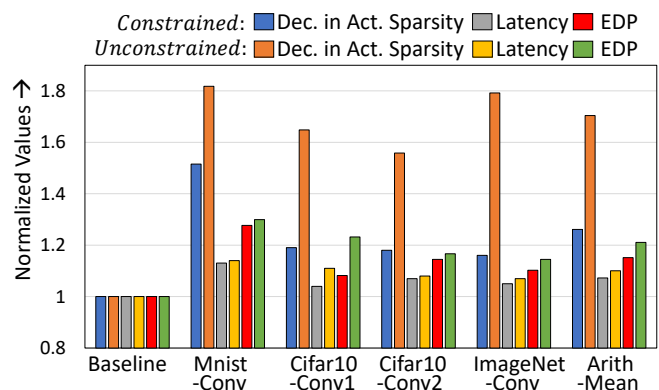


Fig. 20: Impact of adversarial sparsity attacks on activation sparsity, execution time and EDP on SPARCE

In this subsection, we analyze the impact of the sparsity attack on a sparsity-optimized general purpose processor, SparCE. For the sake of brevity, we consider the impact of the white-box attack alone, and depict the resulting increases in latency and EDP in Figure 20. The increase in latency is $1.04\times-1.14\times$, and the increase in EDP is $1.08\times-1.30\times$ - clearly lower than the increase in latency and EDP affected on the Cnvlutin accelerator. We attribute this to the fact that general-purpose processor based platforms derive lower benefits from sparsity in the first place due to overheads such as control instructions for

pointer arithmetic, loop counters, *etc.* Thus, it is not surprising that they tend to show lower vulnerability to the sparsity attacks compared to hardware accelerators.

VII. CONCLUSION

We present a new class of adversarial attacks that adversely impact the execution time and energy consumption of DNNs on sparsity-optimized platforms by introducing input perturbations that cause a reduction in activation sparsity. The proposed sparsity attacks differ from conventional accuracy-based attacks as they do not affect classification accuracy, and can be launched in both white and black-box settings. Across our suite of 4 DNNs on 3 datasets, we achieve a $1.16\times-1.82\times$ decrease in activation sparsity for no loss in classification accuracy. We also demonstrate the impact of our attack on a sparsity-optimized DNN accelerator, achieving a $1.12\times-1.59\times$ increase in latency and a $1.18\times-1.71\times$ increase in EDP.

REFERENCES

- [1] K. He et al. Deep residual learning for image recognition. *CoRR*, abs/1512.03385, 2015.
- [2] Awni Y. Hannun et al. Deep speech: Scaling up end-to-end speech recognition. *CoRR*, abs/1412.5567, 2014.
- [3] G. Hinton et al. Deep neural networks for acoustic modeling in speech recognition: The shared views of four research groups. *IEEE Signal Processing Magazine*, 29(6):82–97, Nov 2012.
- [4] Song Han et al. Deep compression: Compressing deep neural networks with pruning, trained quantization and Huffman coding. 10 2016.
- [5] A. Parashar et al. SCNN: An Accelerator for Compressed-sparse Convolutional Neural Networks. *SIGARCH Comput. Archit. News*, 45(2):27–40, June 2017.
- [6] J. Albericio et al. Cnvlutin: Ineffectual-neuron-free deep neural network computing. In *ISCA 2016*, pages 1–13, June 2016.
- [7] Y. Chen, T. Yang, J. Emer, and V. Sze. Eyeriss v2: A flexible accelerator for emerging deep neural networks on mobile devices. *IEEE Journal on Emerging and Selected Topics in Circuits and Systems*, 9(2):292–308, 2019.
- [8] S. Sen et al. SparCE: Sparsity Aware General-Purpose Core Extensions to Accelerate Deep Neural Networks. *IEEE Transactions on Computers*, 68(6):912–925, June 2019.
- [9] A. Gondimalla et al. Sparten: A sparse tensor accelerator for convolutional neural networks. In *Proc. MICRO*, page 151–165, 2019.
- [10] K. Hegde et al. Extensor: An accelerator for sparse tensor algebra. In *Proc. MICRO*, page 319–333, 2019.
- [11] Maohua Zhu et al. Sparse tensor core: Algorithm and hardware co-design for vector-wise sparse neural networks on modern gpus. In *Proc. MICRO*, page 359–371, 2019.
- [12] Karen Simonyan and Andrew Zisserman. Very deep convolutional networks for large-scale image recognition. *CoRR*, abs/1409.1556, 2014.
- [13] Self driving car reaction time. <http://news.mit.edu/2019/how-fast-humans-react-car-hazards-0807>.
- [14] Alex Krizhevsky, Vinod Nair, and Geoffrey Hinton. Cifar-10 (canadian institute for advanced research).
- [15] Alexey Kurakin, Ian J. Goodfellow, and Samy Bengio. Adversarial examples in the physical world. *CoRR*, abs/1607.02533, 2016.
- [16] Yaniv Taigman et al. Deepface: Closing the gap to human-level performance in face verification. In *Proceedings of the 2014 IEEE Conference on Computer Vision and Pattern Recognition, CVPR '14*, page 1701–1708, USA, 2014. IEEE Computer Society.
- [17] Tom B. Brown et al. Language models are few-shot learners, 2020.
- [18] N. Carlini et al. Towards evaluating the robustness of neural networks. In *2017 IEEE Symposium on Security and Privacy (SP)*, pages 39–57, May 2017.
- [19] Y. Dong et al. Discovering adversarial examples with momentum. *CoRR*, abs/1710.06081, 2017.
- [20] Pin-Yu Chen et al. ZOO. *Proceedings of the 10th ACM Workshop on Artificial Intelligence and Security - AISec '17*, 2017.
- [21] C. Guo et al. Simple black-box adversarial attacks. *CoRR*, abs/1905.07121, 2019.
- [22] Nicolas Papernot et al. Practical black-box attacks against deep learning systems using adversarial examples. *CoRR*, abs/1602.02697, 2016.
- [23] V. Duddu et al. Stealing neural networks via timing side channels. *CoRR*, abs/1812.11720, 2018.
- [24] Reza Shokri et al. Membership inference attacks against machine learning models. *CoRR*, abs/1610.05820, 2016.
- [25] D. Palossi. Ultra low power deep-learning-powered autonomous nano drones. *CoRR*, abs/1805.01831, 2018.
- [26] I. Sutskever et al. On the importance of initialization and momentum in deep learning. In *ICML 2013, ICML'13*, page III–1139–III–1147. JMLR.org, 2013.
- [27] Y. Liu et al. Delving into transferable adversarial examples and black-box attacks. *CoRR*, abs/1611.02770, 2016.
- [28] I. J. Goodfellow et al. Explaining and harnessing adversarial examples, 2014.
- [29] Ian J. Goodfellow, Jonathon Shlens, and Christian Szegedy. Explaining and harnessing adversarial examples, 2014.
- [30] Aleksander Madry, Aleksandar Makelov, Ludwig Schmidt, Dimitris Tsipras, and Adrian Vladu. Towards deep learning models resistant to adversarial attacks, 2017.
- [31] C. Guo et al. Countering adversarial images using input transformations. *CoRR*, abs/1711.00117, 2017.
- [32] Martín Abadi et al. TensorFlow: Large-scale machine learning on heterogeneous systems, 2015. Software available from tensorflow.org.
- [33] Pouya Samangouei, Maya Kabkab, and Rama Chellappa. Defense-gan: Protecting classifiers against adversarial attacks using generative models. *CoRR*, abs/1805.06605, 2018.
- [34] U. Hwang, J. Park, H. Jang, S. Yoon, and N. I. Cho. Puvae: A variational autoencoder to purify adversarial examples. *IEEE Access*, 7:126582–126593, 2019.
- [35] Yann LeCun and Corinna Cortes. MNIST handwritten digit database. 2010.
- [36] J. Deng, W. Dong, R. Socher, L.-J. Li, K. Li, and L. Fei-Fei. ImageNet: A Large-Scale Hierarchical Image Database. In *CVPR09*, 2009.
- [37] J.T. Springenberg et al. Striving for simplicity: The all convolutional net. In *ICLR (workshop track)*, 2015.